sustainability

MDPI

Review

Recent Research in Solar-Driven Hydrogen Production

Yimin Deng [1], Shuo Li [2], Helei Liu [1], Huili Zhang [2] and Jan Baeyens [3,*]

[1] School of Chemistry and Chemical Engineering, Beijing Institute of Technology, Beijing 102488, China
[2] School of Life Science and Technology, Beijing University of Chemical Technology, Beijing 100029, China
[3] Process Technology and Environmental Lab, Department of Chemical Engineering, KU Leuven, 2860 Sint-Katelijne-Waver, Belgium
* Correspondence: baeyens.j@gmail.com

Abstract: Climate concerns require immediate actions to reduce the global average temperature increase. Renewable electricity and renewable energy-based fuels and chemicals are crucial for progressive de-fossilization. Hydrogen will be part of the solution. The main issues to be considered are the growing market for H_2 and the "green" feedstock and energy that should be used to produce H_2. The electrolysis of water using surplus renewable energy is considered an important development. Alternative H_2 production routes should be using "green" feedstock to replace fossil fuels. We firstly investigated these alternative routes through using bio-based methanol or ethanol or ammonia from digesting agro-industrial or domestic waste. The catalytic conversion of CH_4 to C and H_2 was examined as a possible option for decarbonizing the natural gas grid. Secondly, water splitting by reversible redox reactions was examined, but using a renewable energy supply was deemed necessary. The application of renewable heat or power was therefore investigated, with a special focus on using concentrated solar tower (CST) technology. We finally assessed valorization data to provide a tentative view of the scale-up potential and economic aspects of the systems and determine the needs for future research and developments.

Keywords: hydrogen production; "green" systems; solar power; catalytic steam reforming; water splitting; valorization

Citation: Deng, Y.; Li, S.; Liu, H.; Zhang, H.; Baeyens, J. Recent Research in Solar-Driven Hydrogen Production. *Sustainability* **2024**, *16*, 2883. https://doi.org/10.3390/su16072883

Academic Editor: Andrea Nicolini

Received: 21 February 2024
Revised: 25 March 2024
Accepted: 27 March 2024
Published: 29 March 2024

1. Introduction

1.1. Reviewing the Current H_2 Production Routes

The current energy systems are environmentally unsustainable with reduced resources, increasing the world's population and increasing energy use, hampering the energy future. Future energy supplies will need to apply clean and CO_2-lean renewable sources whilst partly decarbonizing the energy sector. Regarding the target objectives, the major energy consumers will be the building, industry, and transportation sectors. The intermittent nature of some renewables (wind, solar) will result in the use of energy storage techniques. Novel techniques will need to be developed to manufacture environmentally friendly energy carriers that can be easily stored and transported [1].

Producing H_2 has a high potential to either decarbonize the natural gas grid [2], to directly drive fuel cells, to reduce iron ore [3], or to fire cement, ceramic, or limestone kilns [4,5]. The current methods used for the production of H_2, namely the reforming of fossil feedstock or H_2 production by "renewable" routes of biomass gasification and carbohydrate fermentation, still release CO_2. These routes have been previously assessed [6]. Novel approaches will deal with "green" feedstock such as CH_4 (digester biogas), NH_3 (stripping of digestate), methanol, and ethanol (fermentations), and even their fossil fuel-based equivalents can be considered. These feedstock materials can mostly be catalytically steam reformed into H_2. The decomposition of CH_4 and NH_3 does not require H_2O addition. Thermal water decomposition by oxidation reduction reactions has been investigated but is not fully proven yet [6].

To reduce CO_2 emissions, Abdin et al. estimate that approximately 1 billion tons of non-fossil-based H_2 is required, 10 times more than the current amount of H_2 produced [7]. Although electrolysis using renewable energy is promoted, the current supplies are insufficient to meet this goal [8].

H_2 is currently mainly (~50%) produced by the steam reforming of natural gas/oil/naphtha. About 30% is covered by the refinery/chemical industry, and coal gasification produces about 18%. Water electrolysis (3.9%) and other minor sources make up the rest of the annual H_2 production. In the future, "green" H_2 processes will need to supply H_2 for traditional and new applications [9,10].

The current H_2 applications are mainly in oil refineries and in chemicals' syntheses, from the hydrogenation of fats/oils to the manufacturing of pharmaceuticals, among others. The future is expected to enhance the demand for H_2 for both chemical processes and for transportation fuel.

The different current ways to produce H_2 have limitations and advantages, as summarized in Table 1 [11,12]. The tentative cost of H_2 varies among the processes, which have different levels of maturity. The specific case of electrolysis is illustrated in Table 2.

Table 1. Characteristics of H_2 generation methods.

H_2 Production Methods	**H_2 Cost USD/kg H_2**	**Advantages**	**Drawbacks**
Auto-thermal reforming	1.5	➢ Low operating temperature. ➢ Limited methane slip.	➢ Air is required. ➢ O_2/CO_2—byproducts.
Partial oxidation	1.5	➢ No catalyst needed. ➢ Requires a lower degree of feedstock desulfurization. ➢ Limited methane slip.	➢ Low H_2/CO ratio. ➢ Soot formation. ➢ High operating temperature.
Steam reforming	3–5	➢ Mature technology. ➢ No O_2 needed. ➢ Lower operating temperature. ➢ Highest H_2/CO ratio.	➢ High production of CO. ➢ High production of CO_2.
Gasification/pyrolysis	1.6–2.1	➢ Nearly CO_2-neutral. ➢ Abundant. ➢ Cheap biomass feedstock.	➢ Variable H_2 yield. ➢ Formation volumes.
Electrolysis	5–7	➢ Zero emission. ➢ O_2—byproduct. ➢ Existing infrastructure.	➢ Currently uses fossil fuel-based electricity.
Water thermolysis	8	➢ Clean and sustainable. ➢ O_2—byproduct. ➢ Abundant feedstock.	➢ Elements toxicity. ➢ Corrosion problems. ➢ High capital costs.
Bio photolysis	1	➢ CO_2 consumed. ➢ O_2—byproduct. ➢ Mild operation conditions.	➢ Lower H_2 yields. ➢ O_2 sensitivity. ➢ Sunlight needed. ➢ Requires large reactor volumes.
Photolysis	8–10	➢ Abundant feedstock. ➢ O_2—byproduct. ➢ No emission.	➢ Low efficiency. ➢ Requires sunlight.

Regarding electrolysis, Table 2 refers to mature alkaline electrolysis [13]. The proton exchange [H^+] polymer electrolyte membrane (H^+-PEM) is ready for commercial application for operation at 20 to 200 °C, with an estimated efficiency of 65 to 82% [14–16]. Solid oxide electrolysis (SOE) processes can reach a 100% efficiency while operating at high temperatures [17]. While the H^+-SOE type is close to the demonstration scale, the O^{2-}-SOE is still at a laboratory scale. The H_2 production costs associated with H^+-PEM and SOE have not yet been fully determined, but cheap photovoltaic or curtailed wind energy (<0.02 USD/kWh) will be required to achieve costs between 1.4 and 1.7 USD/kg H_2. The required 0.02 USD/kWh is far below the current cost.

Table 2. Characteristics of electrolysis systems for H_2 generation.

Technology **Technology Maturity**	**Alkaline [13]** **Mature**	**PEM [14]** **Demonstration**	**SOE [18]** **R&D**
Temperature, °C	60–80	50–80	500–1000
Pressure, bar	<30	<30	<30
Energy consumption, kWh/Nm^3	4.5–7.0	4.5–7.5	2.5–3.5
Surface area of the cells, m^2	<4	<300	-
H_2 yield, Nm^3/h	<760	<30	-
Tentative lifetime, yr	20–30	10–20	-
Hydrogen quality, %	>99.8	>99.99	-

1.2. The Current Development of Electrolysis

Although only responsible for ~4% of the current amount of H_2 produced, electrolysis developments are important. Whatever developments are selected, the process will require cheap electricity and should hence be considered in conjunction with nuclear power, curtailed PV or wind power, or concentrated solar power. The construction of the process electrodes is a major research topic. De-ionized water is required before electrolysis, and catalysts (e.g., platinum) will be required. The reaction is straightforward and will decompose water (liquid) into H_2 (g) and O_2 (g) at an E_0 value of −1.229 V.

The current cost of H_2 production through electrolysis largely exceeds the cost of the reforming production methods, and future progress is only guaranteed if the electrolysis process applies cheap renewable electricity. Table 2 summarizes water electrolysis developments.

The immediate future of green electrolytic H_2 relies mostly on wind or photovoltaic electricity despite the high specific energy required [8]. The further growth of electrolysis will not be capable of meeting the expected 1-billion-ton H_2 goal. Fossil-based feedstock will hence remain the dominant H_2 source despite the CO_2 emissions of about 10 kg of CO_2/kg H_2 for steam methane reforming ("gray hydrogen") [19]. The technology could be "cleaner" if carbon capture and storage were applied. This would, however, involve significant costs, nearly double the produced H_2 costs [20].

2. Current Hot-Topic H_2 Production Methods

2.1. Thermal Single-Step Water Splitting

Water can be thermally dissociated (water thermolysis) in H_2 (g) and 0.5 O_2 (g). To achieve a fair water dissociation, high temperatures above 2500 K are required [21]. Moreover, the process requires the efficient separation of H_2 and O_2 to avoid explosion hazards. Membranes with, e.g., ZrO_2 can be used up to 2500 K. Separation can also be achieved at low temperatures after quickly (millisecond level) quenching the product gas mixture to below 500 K, where Palladium membranes can be efficiently used. Only nuclear or concentrated solar towers can meet the required high temperatures, but the selection of usable high-temperature construction materials remains a major bottleneck [22].

2.2. Thermo-Chemical Redox Water Splitting

Most of the thermo-chemical redox cycles published to date belong to one of five generic cycles shown in Table 3 and Figure 1 [23,24]. M is either in pure metal form or its lower valency cation in an oxide or halide pair.

Table 3. Thermo-chemical redox H_2 cycles.

Types	Number of Steps in the Complete Cycle
Type 1: Metal–metal oxide	Two
Type 2: Metal oxide–metal oxide	Four
Type 3: Metal oxide–metal hydroxide	Three
Type 4: Metal oxide–metal sulfate	Three
Type 5: Metal–metal halide	Three
Type 6: Metal oxide–metal halides	Four

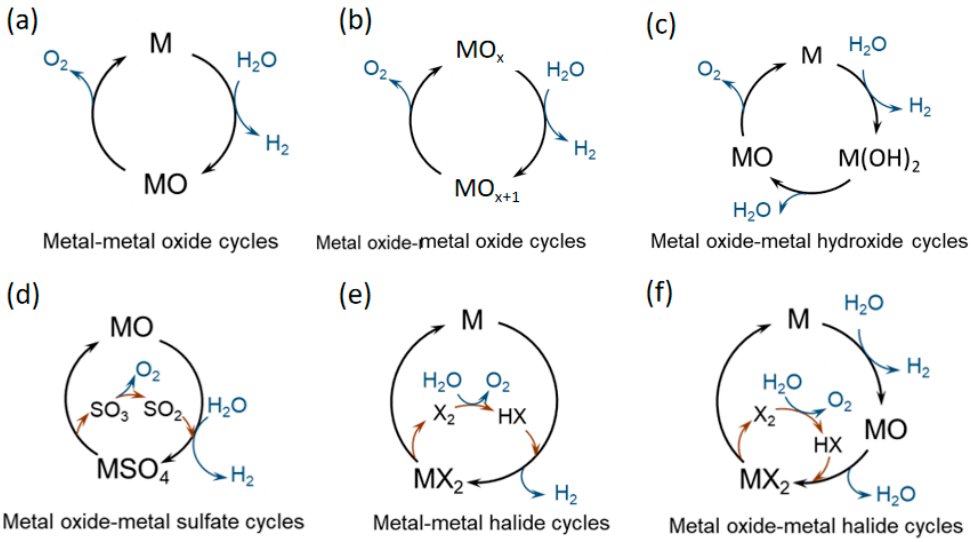

Figure 1. Current thermo-chemical H_2 production cycles according to the types of Table 1. (**a**) metal-metal oxide; (**b**) metal oxide-metal oxide cycles; (**c**) metal oxide-metal hydroxide cycles; (**d**) metal oxide-metal sulfate cycles; (**e**) metal-metal halide cycles; (**f**) metal oxide-metal halide cycles.

The simpler schemes are desirable in terms of efficiency and capital cost. Only a few redox cycles can operate below a temperature of 1000 K. Many compounds form multi-step cycles and require a high operating temperature. Moreover, the incomplete reversibility reduces the process efficiency [23,24]. Possible developments are further discussed in subsequent sections.

2.3. Conversion of Methane (or Hydrocarbons)

Commercial bulk H_2 is commonly produced from methane or hydrocarbons. These processes have a long history (>50 years). Steam methane reforming (SMR) operates at 700 to 1100 °C over a metal-based catalyst (nickel). Steam reacts with methane to produce CO and H_2.

$$CH_4 + H_2O \rightarrow CO + 3H_2$$

$$CO + H_2O \rightarrow CO_2 + H_2$$

Both reactions are reversible [25], and the process efficiency is between 65 and 75%. The CO_2 must be abated. The alternative, the direct conversion of CH_4, requires temperatures above 1500 K. The occurring reactions are given below.

2.4. Methanol to Hydrogen

Due to the difficulties in transporting and handling H_2, methanol, containing 12.6 wt% of H, is considered as a cheap and abundant feedstock. Although methanol is mostly produced by chemical synthesis, new "green" production methods have emerged through biochemical methods.

2.5. NH_3 to Hydrogen

The reversible decomposition reaction of ammonia follows the below-listed equation:

$$NH_3 \leftrightarrow 0.5\ N_2 + 1.5\ H_2\ \Delta H_0 = 46.2\ kJ/mol$$

The decomposition reaction is mildly endothermic and needs a catalyst to lower the activation energy. Many possible catalysts can be used for this reaction. Several catalysts were investigated in the present study, and we will report the function of different temperatures and reaction times. Details are reported in Section 4.

2.6. Objectives of the Research

Further reported research will also demonstrate that fairly low-temperature catalytic steam reforming is possible, as initially proposed in [25,26].

The results of our research demonstrate that decentralized H_2 production from transportable and cheap CH_3OH is possible in a low T, P process using durable and selective nanoparticle-based catalysis, with low-to-no CO being produced. This method has potential applicability in the transportation of fuel cells. Finally, redox-driven water splitting will be illustrated, together with some recent developments in using concentrated solar heat to meet endothermic reaction requirements.

3. Solar H_2 Production

3.1. Near-Term Options

Since all conversion processes are endothermic, a cheap energy source is required, with wind and solar energy being used in the energy supply of endothermic reactions. Figure 2 and Table 4 illustrate the different routes for producing H_2 by thermolysis, electrolysis, and photonic dissociation. Concentrated solar power (CSP) systems can be applied in the solar production of H_2. Figure 2 illustrates how concentrated solar radiation can be used in the solar production of H_2 from water or carbonaceous materials.

Water, as an abundant and cheap reactant, should be the ultimate H_2 feedstock. It is carbon-free and can be decomposed through solar-driven water splitting by thermochemical redox cycles. Its large-scale application will depend upon the achievement of a fairly low temperature and multi-cycle reversibility [18,27]. Since solar-driven systems still suffer from a low cost-effectiveness and intermittency, novel solutions are required to increase their efficiency and provide a considerable cost reduction [28]. Even in solar–thermal applications, the catalytic steam reforming of low-cost biochemicals such as bioethanol has a high potential, with a H_2 production efficiency exceeding 95%.

Table 4 summarizes the characteristics of different reported solar H_2 processes. Although full data have not yet been given, a positive appraisal emerges from the comparison. These processes can foster the future production of "green" hydrogen.

Moreover, it should not be forgotten that hybrid solar PV and on/offshore wind systems are currently being investigated, demonstrating that the cost in USD/kg H_2 will exceed the current petrochemical production costs, except in parts of the world with a high PV and wind electricity potential. This is illustrated in Figure 3.

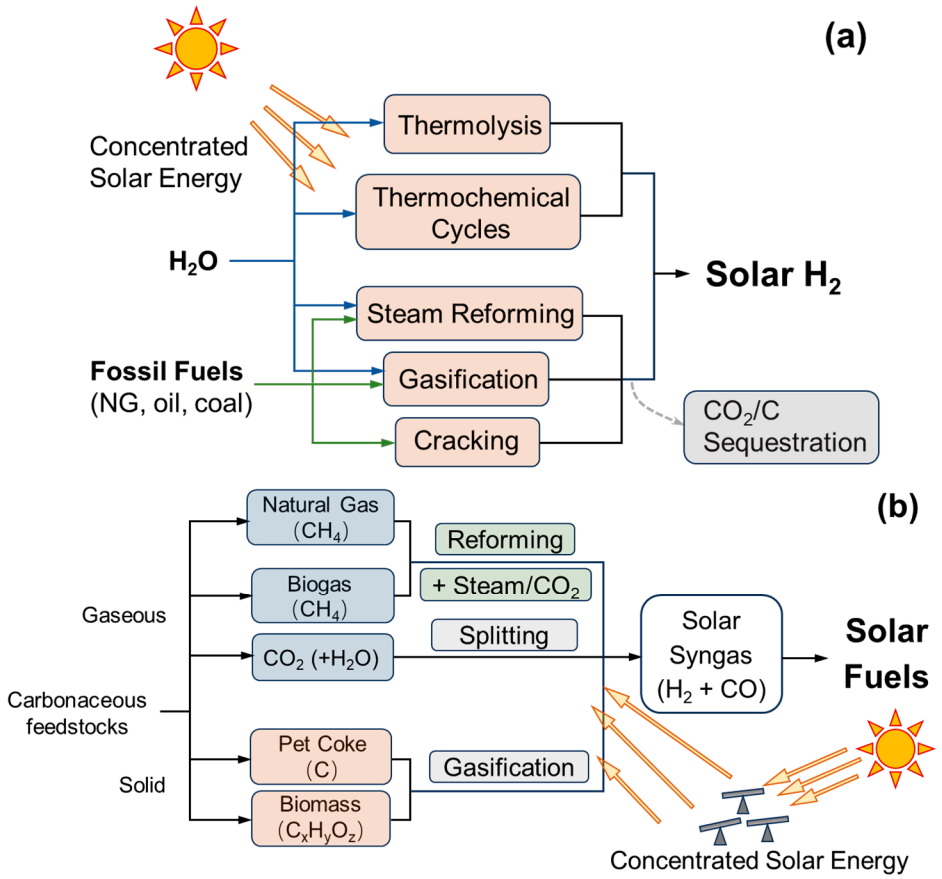

Figure 2. Solar-aided routes to produce H_2, with (**a**) from water and fossil fuels; and (**b**) carbonaceous gases or solid feedstock.

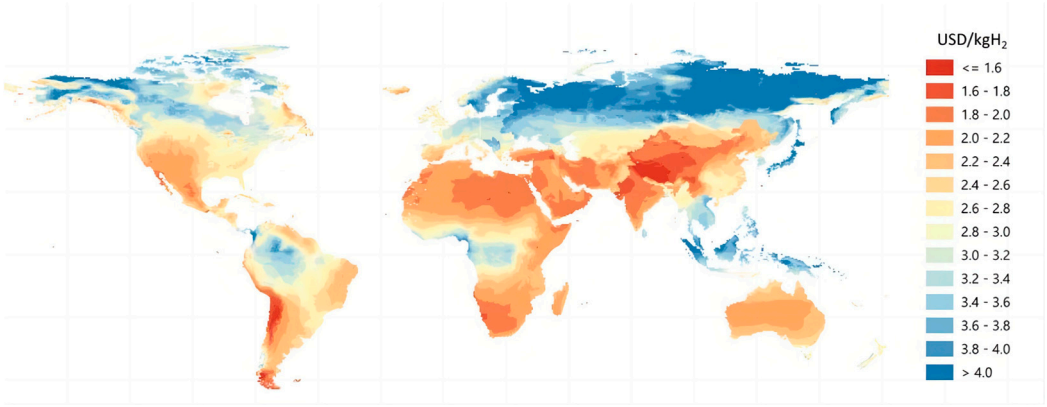

Figure 3. Expected H_2 costs from hybrid solar PV and onshore wind systems. Reproduced by IEA; 2019; The Future of Hydrogen—Seizing today's opportunities; https://www.iea.org/reports/the-future-of-hydrogen, accessed on 4 January 2024, License: [CC BY 4.0] [43].

3.2. The Concentrated Solar Tower Solution

Concentrated solar energy is of increasing interest in power and industrial heat generation. The intermittency of solar energy necessitates the integration of a heat storage system to operate on a continuous basis. The applications of different CSP technologies are mainly a function of the targeted temperature ranges and the intended applications, as illustrated in Figure 4.

Table 4. Characteristics of developed solar H_2 production techniques.

Solar System	Reqd. T	Type	Feed	CO_2 Product	System Efficiency (%)	Capacity, (ton H_2/d)	H_2 Price, (USD/kg)
Concentrated solar thermal							
Solar tower [29–31]	Low	Electrolysis (PEM)	Water	No	21	38.35	5.1
	High	Thermolysis	Coal	CCS-integrated	38–40	-	-
Solar dish [32]	High	Steam electrolysis	Water	No	20	1.36	10.5
Parabolic trough [32]	High	Steam electrolysis	Water	No	20	62.95	6.5
Concentrated solar tower [33–35]	High	Thermochemical cycle	Hydrocarbons	No	-	6	8.0
	High	Thermochemical cycle	Water/CO_2	No	4.1	-	-
	High	Thermochemical cycle	Water/CO_2	No	22.8–39.6	-	-
Concentrated solar tower [4,36]	High	Thermolysis	Water	No	29.9	3320 L/h	
	High	Gasification	Solid carbonaceous (e.g., coal)	Yes	-	-	-
	High	Pyrolysis	NG, oil, and hydrocarbons	Yes	-	-	-
	High	Steam reforming	NG, oil, and hydrocarbons	Yes	-	-	-
	High	Thermolysis	Water	No	5.6	-	-
PV [28]	Low	Electrolysis (PEM)	Water	No	9.8	10	12.1
Photo-electrochemical [37]	High	Photo-catalysis	Water	No	-	-	-
Solar power plant [38]	High	Solar power	Water	No	24.9	-	-
Hybrid systems [31,38–41]							
Solar thermal [42]	High	Electrolysis (PEM)	Water	No	10	71	6.3
PV–grid [28]	Low	Electrolysis (PEM)	Water	No	9.8	10	6.1
PV–thermal [39,41]	High	Thermolysis	Water	No	-	-	-
	High	Thermolysis	Various	Limited	-	-	-
PV–CSP [30]	High	Thermolysis	Water	No	-	-	2.7
Solar and wind [40]	High	Electrolysis	Various	Limited	-	-	-

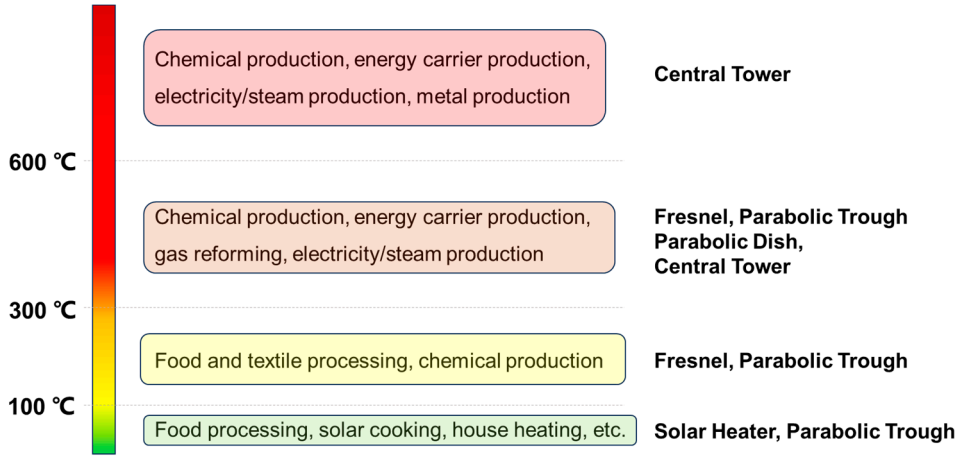

Figure 4. Temperature ranges and application areas of various CSP technologies.

For solar power applications, both parabolic trough and central tower concepts are mostly used, with parabolic troughs being responsible for most of the moderate temperature thermodynamic cycles. Central tower concepts, however, have gained importance as Peaker solutions since new heat transfer media (i.e., particle suspensions) enable a higher temperature application, hence fostering the use of high-efficiency thermodynamic cycles.

Such a particle-driven concept has been developed over the past few years with a particle loop operation at a temperature around 800 °C. A vertical multi-tube (40) solar receiver reached a capture yield of >2 MW_{th}. The future scale-up to between 10 and 50 MW_{th} will apply the same multi-tube layout with taller tubes of ≥6 m.

4. Experimental Investigation of H_2 Production from "Gray" or "Green" Feedstock

Four experimental set-ups were used, each of which are depicted in Figure 5. The reactors contained fixed or vibro-fluidized beds of the appropriate catalyst particles (15 cm bed depth for the fixed bed mode in the electrical furnaces and 25 cm in the sun-heated fluidized bed reactor). The general layout of the experiments is given in Figure 5a, while equipment details are given in Figure 5b–e. Details of the rigs are presented in Deng et al. [2,44].

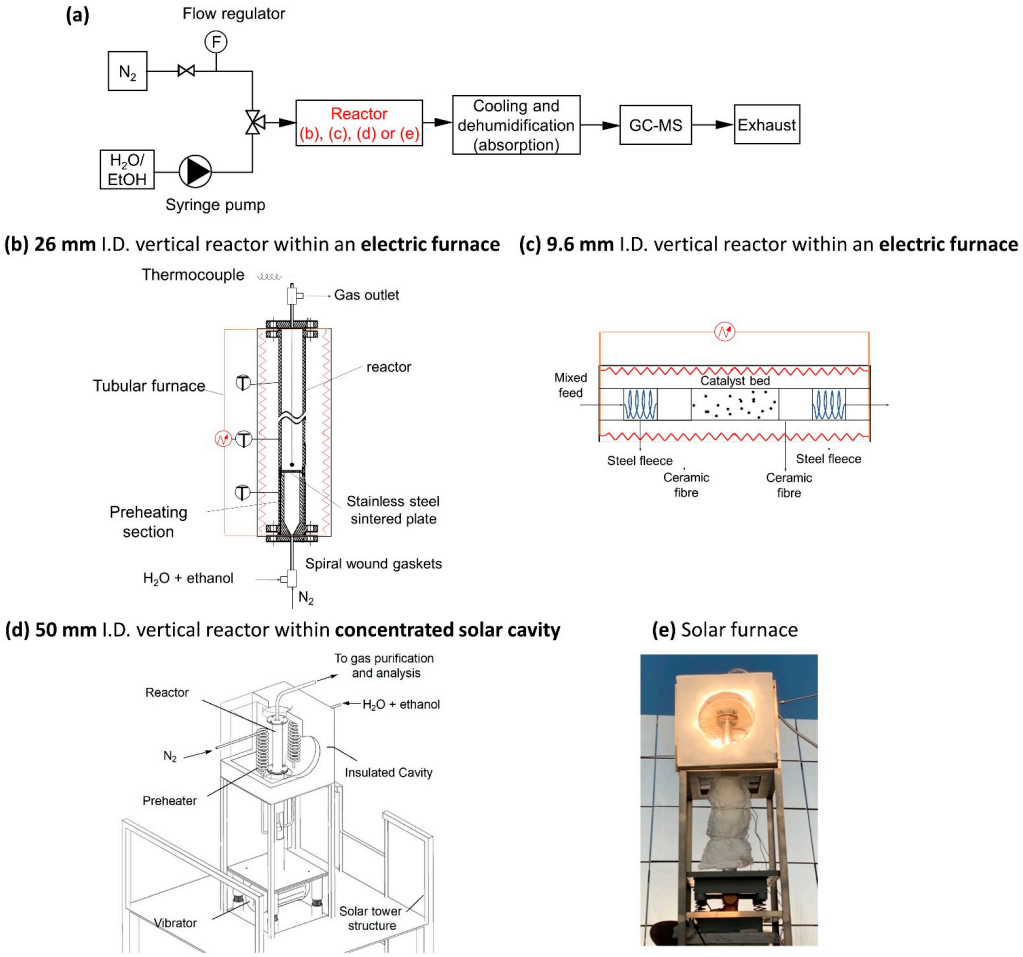

Figure 5. Experiments: (**a**) overall layout, (**b**) 26 mm I.D. vertical electrically heated reactor, (**c**) 9.6 mm I.D. horizontal electrically heated reactor, (**d**) fluidized bed reactor (50 mm I.D.) in the solar cavity, and (**e**) illustration of the reactor depicted in (**d**).

The first "gray" feedstock, CH_4, was investigated mostly for its hydrogen-enhanced natural gas (HENG) potential. Our experimental investigation applied wet-impregnated Fe/α-Al_2O_3 and Ni/MgO catalysts. The 20 wt% Fe/α-Al_2O_3 catalyst yields nearly complete CH_4 conversion at 700 °C and is preferred for CH_4 conversion. Ni/MgO catalysis leads to lower conversions at similar operating conditions (Figure 6). The decomposition carbon accumulates on and within the catalyst, progressively reducing the H_2 yield. A periodic regeneration (burning off the coke deposit) is required after 20 to 30 h of production. At temperatures below 635 °C, the reaction kinetics are dominated by the reaction rate. Mass transfer limitations are increasingly important at higher temperatures. Figure 6

depicts the conversion effects of reaction time and temperature. The use of the Fe catalyst is recommended.

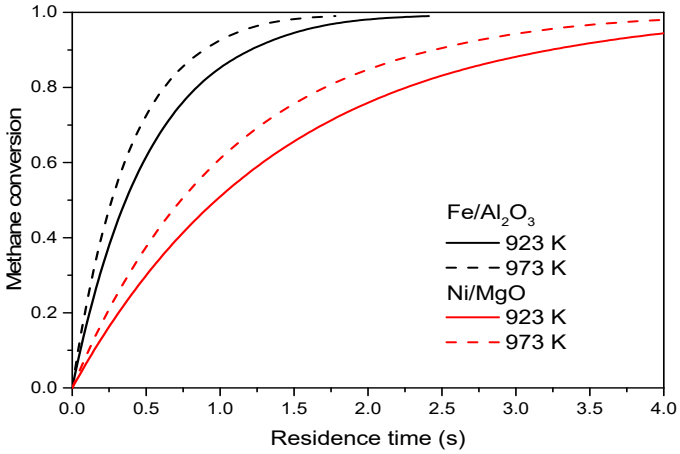

Figure 6. Methane conversion for different residence times at 650 and 700 °C.

A second "gray" feedstock (with the potential to become "green" through future developments in the bio-synthesis of methanol feedstock), CH_3OH, was examined. The experimental results in Figure 7 show that the yield of the catalytic steam reforming of methanol is almost 2.5 mol H_2/mol CH_3OH (slightly lower than the stoichiometric yield of 3 mol H_2/mol CH_3OH). The CH_3OH–carbon is mostly detected as CO and CO_2, as illustrated in Table 5. No coke deposits were detected after long-duration experiments. The catalysts maintained their selectivity and activity. The kinetics demonstrated a high reaction rate. The $MnFe_2O_4$ catalyst is four times slower and also requires a higher conversion temperature (400 °C).

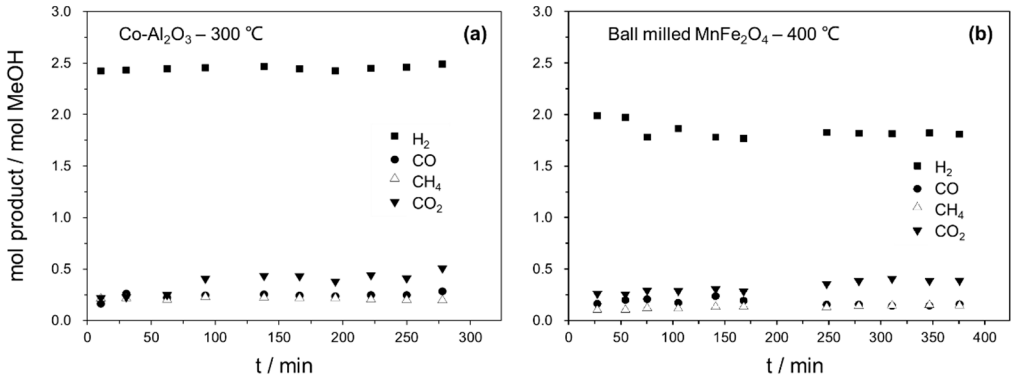

Figure 7. Conversion of methanol with Co/α-Al_2O_3 (**a**) and $MnFe_2O_4$ (**b**) catalysts.

Table 5. Carbon selectivity of steam methanol reforming.

	$MnFe_2O_4$		$Co\text{-}Al_2O_3$
Selectivity (%)	**573 K**	**673 K**	**573 K**
CO	38.12	27.85	29.24
CH_4	5.76	20.54	25.88
CO_2	56.11	51.61	44.88

Using the Co/α-Al_2O_3 catalyst is recommended for scale-up and fuel cell application due to the higher H_2 yield and lower CO formation.

Thirdly, the production of **H_2 from "green" or industrial NH_3** was studied in the present research using non-noble metal catalysts. "Green" ammonia sources were investigated, such as ammonia produced by stripping from manure and digestate. Three catalysts

were tested: wet-impregnated Fe-Al_2O_3, dry-milled Fe-Al_2O_3, and wet-impregnated Ni-Al_2O_3. The results are illustrated in Figure 8. The mildly endothermic decomposition of NH_3 into H_2 and N_2 is achieved with a 100% yield at 500 °C using a Fe/α-Al_2O_3 catalyst. The alternative and more expensive Ni/α-Al_2O_3 catalyst scores significantly lower. The experimental results were converted into reaction kinetics. The reaction is very fast, with a rate constant of 7.5/s at 500 °C. Full conversion is obtained within 0.4 s. Very pure (>95%) H_2 can be produced and stored using several techniques. It is proven that the production of H_2 from NH_3 has a high potential and merits pilot-scale consideration.

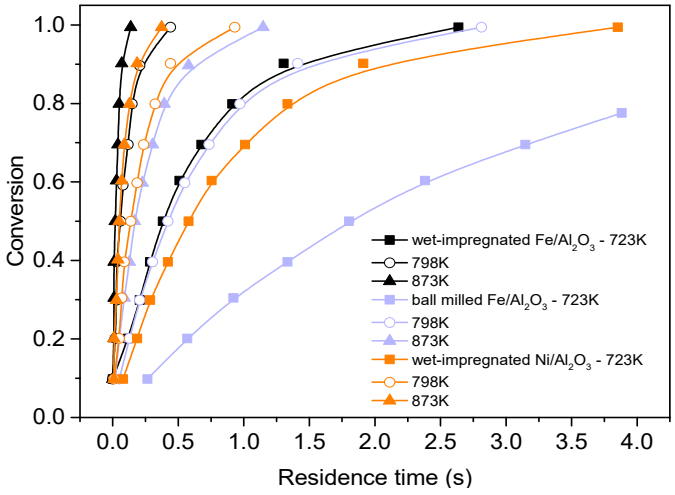

Figure 8. Effect of residence time and temperature on the conversion of NH_3.

For the **Catalytic steam reforming of ethanol (CSRE)**, the most promising catalysts were selected from an in-depth literature review and tested in the present research using all the equipment alternatives in Figure 9, and this test was carried out for more than 30 successive hours. The H_2 production efficiencies (5.5 mol H_2/mol ethanol) were close to the expected stoichiometric values. CO and CO_2 were the main carbon-bearing reaction products. The results are illustrated in Figure 9. A kinetic analysis defined the reaction rate expressions, and the reaction rate per unit catalyst weight was established at 0.58 mol H_2/g_{cat} h. Abundant bio-ethanol can be obtained from first- and second-generation fermentation.

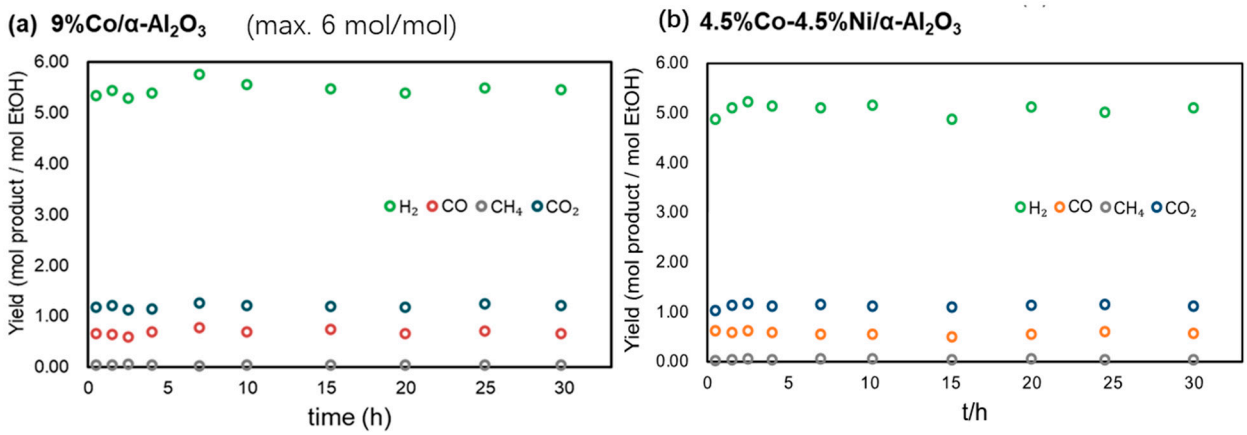

Figure 9. Results for the 9% Co/α-Al_2O_3 and 4.5% Co-4.5%Ni/α-Al_2O_3 catalysts (**a**,**b**).

The average yields, expressed as mol products/mol EtOH, for 30 h of continuous operation were 5.463 ± 0.306 for H_2, 0.670 ± 0.103 for CO, 0.038 ± 0.012 for CH_4, and 1.196 ± 0.063 for CO_2 in the operation mode of Figure 9a. For the operation mode of Figure 9b, the results were 5.149 ± 0.276 for H_2, 0.579 ± 0.073 for CO, 0.047 ± 0.024 for CH_4, and 1.123 ± 0.100 for CO_2.

5. Water Splitting by Redox Reactants

While water splitting by thermolysis occurs at very high temperatures, redox-driven water splitting cycles can operate at moderate temperatures. Based on previous studies in the literature, 24 investigated cycles, mostly investigated by small-scale experiments, were examined by a multi-criteria decision-making exercise [18]. From the objective screening, the priority redox systems selected used MnO_x/Na_2CO_3 and $MnFe_2O_4/Na_2CO_3$. These systems were those further investigated for short- and long-duration cycling [18].

The thermochemical cycle of $MnFe_2O_4/Na_2CO_3$ is generally described by the following reactions:

$$2MnFe_2O_4(s) + 3Na_2CO_3(s) + H_2O(g) \rightarrow 6Na(Mn_{1/3}Fe_{2/3})O_2(s) + 3CO_2(g) + H_2(g)$$

$$6Na(Mn_{1/3}Fe_{2/3})O_2(s) + 3CO_2(g) \rightarrow 2MnFe_2O_4(s) + 3Na_2CO_3(s) + 0.5O_2(g)$$

The thermochemical cycle of MnO_x/Na_2CO_3 is generally described by the following reactions:

$$3Na_2CO_3(s) + 2Mn_3O_4(s) \rightarrow 4NaMnO_2(s) + 2CO_2(g) + 2MnO(s) + Na_2CO_3(s)$$

$$2MnO(s) + Na_2CO_3(s) + H_2O(v) \rightarrow H_2(g) + CO_2(g) + 2NaMnO_2(s)$$

$$6NaMnO_2(s) + ayH_2O(v) + (3+b)CO_2(g) \rightarrow 3Na_2CO_3(s) + aH_xMnO_2{\cdot}yH_2O(s) + bMnCO_3(s) + cMn_3O_4(s)$$

$$aH_xMnO_2{\cdot}yH_2O(s) + bMnCO_3(s) \rightarrow (2-c)Mn_3O_4(s) + ayH_2O(v) + bCO_2(g) + 0.5O_2(g)$$

For the **MnO_x/Na_2CO_3** redox water splitting system, tests were carried out in the electrical furnace (Figure 5b) and in the solar furnace (Figure 5d) at 775 and 825 °C, with 10 and 250 g of redox reactant, respectively. Solar results are illustrated in Figure 10. Milled particles (<1 µm) with a large surface area provide better results. Ten complete oxidation/reduction cycles were tested. The cumulative H_2 production achieved 78% at 825 °C. Milled Mn_3O_4/Na_2CO_3 reached a yield of over 80% in the first cycle and over 77% after 10 cycles. The Mn_3O_4/Na_2CO_3 system obtained an efficiency of >95% at 775 °C in the solar furnace despite the high T required, but provided that cheap thermal energy could be supplied, over 100 cycles are needed to reach H_2 production costs below 2 EUR/kg. The separation and reused of CO_2 in the multi-step reaction system remain a major drawback.

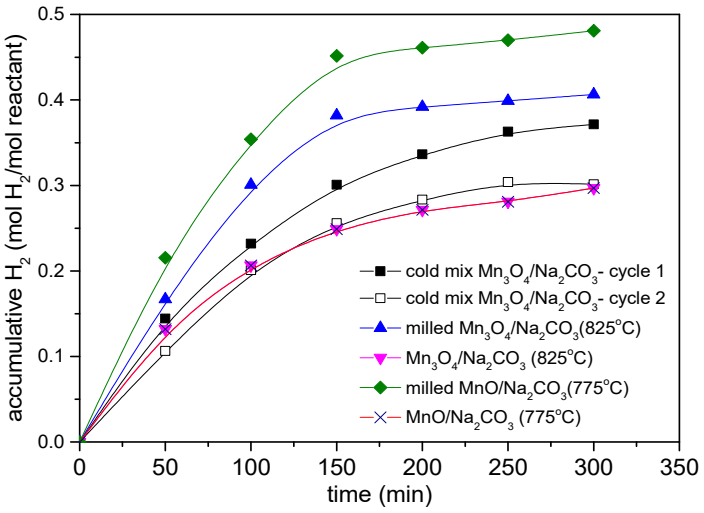

Figure 10. H_2 yields using the MnO_x/Na_2CO_3 cycle in the solar furnace.

The **$MnFe_2O_4/Na_2CO_3$ cycles** were isothermally tested for more than 200 successive cycles by thermogravimetry in the electric furnace and in the solar reactor. A H_2 production efficiency in excess of 85% was obtained with the co-precipitated reactant after multiple

cycles. The results are presented in Figure 11. Our solar tests confirmed >95% H_2 efficiency. The reverse CO_2 reaction time should exceed 4.5 h; 6 h is preferable. The CO_2 for the regeneration step was introduced after each oxidation (H_2 release) step. CO_2 was not recovered in the experiments, and bottled CO_2 was used. The preliminary results with a reduction step of 3 h [45] demonstrated that the regeneration was incomplete. Only a regeneration duration of 4.5 (preferably 6) hours could nearly regenerate the redox reactant and achieve a high H_2 yield after multi-cycle reactions. Tentative economic calculations revealed that 120 consecutive cycles would produce H_2 at 1 EUR/kg H_2. However, this is only possible if a cheap energy supply is available and if CO_2 can be fully reused in the reduction reaction. The 30% cheaper ball-milled reactant will proportionally reduce costs. The obtained results demonstrate that the further improvement of the system is important.

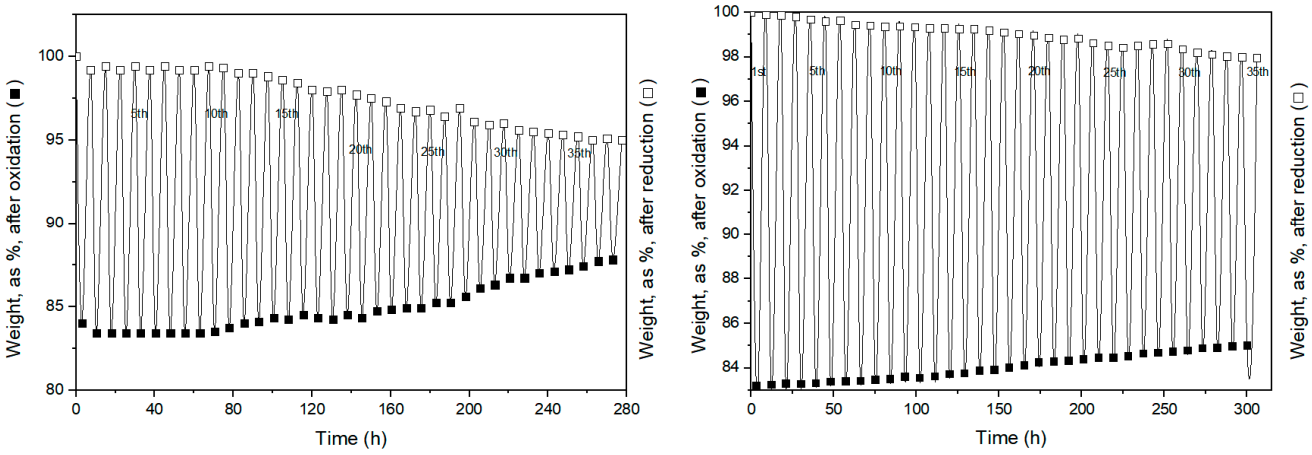

Figure 11. Redox cycle experiments (reproduced from [45], courtesy of RSC Advances). (**a**) Weight changes in the oxidation (3 h) and reduction cycles (4.5 h), respectively. (**b**) Weight changes in the oxidation (3 h) and reduction cycles (6 h), respectively.

The H_2 production efficiency can largely exceed 90% when appropriate oxidation and reduction times are applied. Co-precipitated $MnFe_2O_4$ costs ~500 EUR/ton, as opposed to ~350 USD/ton for the ball-milled alternative.

Both the use of renewable energy and good heat management amongst the cycles of the system are important for limiting heating costs. Since CO_2 is required in the reverse reaction, it should be fully recovered. The proposed $MnFe_2O_4/Na_2CO_3$ cycle needs further testing at pilot scale to really prove its competitiveness with other H_2 production methods with the electrolysis of water using solar-based electricity or heat. Pilot- and commercial-scale experiments are required to confirm lab-scale results.

6. Valorization Potential

In this section, special attention is paid to the scale-up and Technology Readiness Level of the investigated H_2 production technologies, their costs, and associated process requirements, such as H_2 upgrading, the potential solid oxide fuel cell applications, and additional technical matters. Essential findings are summarized and used in scale-up procedures for both the thermo-catalytic conversion of CH_4, CH_3OH, C_2H_5OH, and NH_3 and for $MnFe_2O_4/Na_2CO_3$ redox water splitting. The additional topics of H_2 upgrading, the safety issues associated with H_2 production and its use, and high-temperature gas filtration are discussed. A techno-economic assessment and a tentative discussion of the Technology Readiness Level (TRL) will be presented. Finally, the solar receivers will be briefly discussed according to their temperature classification.

Thermo-catalytic H_2 production: The experimental results provided design equations and methods for these reaction systems. However, a distinction needs to be made between

the CH_4 feedstock and the CH_3OH, NH_3, and C_2H_5OH feedstock. In the case of CH_4, coking is a major issue, with the catalyst being progressively de-activated if not thermally regenerated. The reaction temperatures are also moderate to high. The catalyst is an A-type particle, meaning it is easily fluidized and conveyed. No H_2O is required. In the other cases, no coking is observed, and low (250 °C) to moderate (500 °C) temperatures are required. The catalyst is, however, of µm grade. This results in very high reaction rates, near-complete conversions at short contact times, and high gas hourly space velocities (GHSVs), as listed in Table 6.

Table 6. Gas hourly space velocities (GHSVs) of different hydrogen production systems.

System	GHSV
NH_3	10 L H_2 h^{-1} $kg_{cat}{}^{-1}$
CH_3OH	900 L H_2 h^{-1} $kg_{cat}{}^{-1}$
C_2H_5OH	13,000 L H_2 h^{-1} $kg_{cat}{}^{-1}$

Small amounts of catalyst can generate significant amounts of H_2. These differences will significantly affect the scale-up potential, as illustrated below. In view of the catalyst size, a fluidized bed (CH_4, NH_3) or a fixed bed (methanol, ethanol) were proposed and studied using different plant layouts. The main layout is depicted in Figure 12.

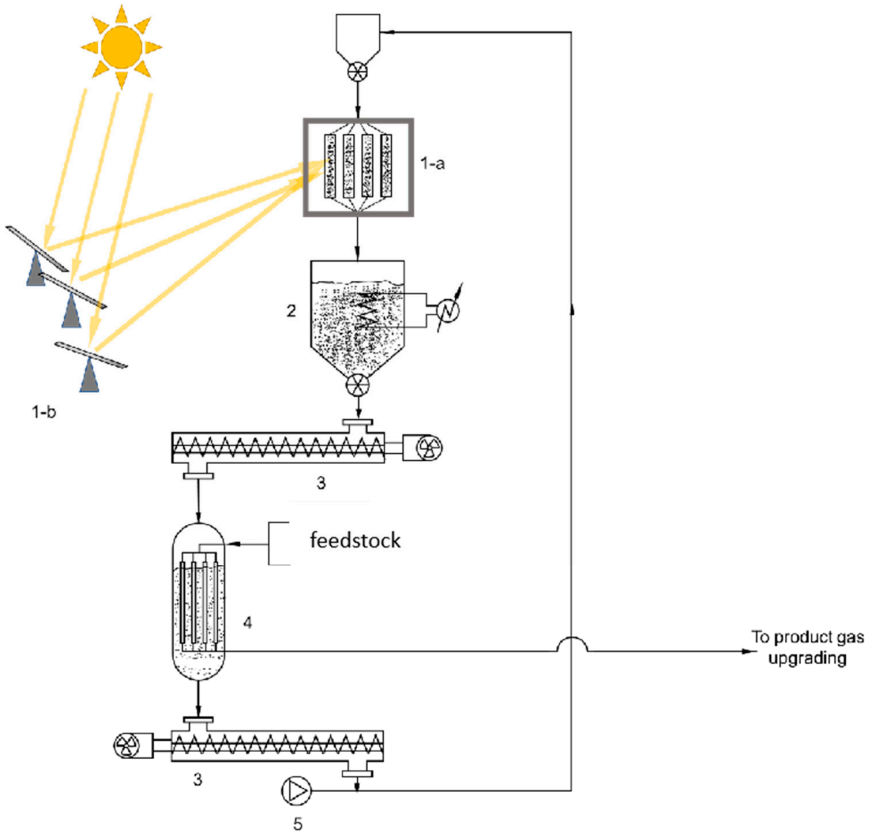

Figure 12. Layout of the experimental set-up. 1. Solar Cavity Receiver 1-a (with associated heliostats 1-b) and either vertical or horizontal fluidized bed particle carrier heating. 2. Hot particle carrier storage with possibly supplementary heating from PV or wind turbine (or waste heat). 3. Free-bearing screw conveyors. 4. Moving-bed indirect conversion reactor (multi-tubular catalyst bed). 5. Recycling of carrier particles to 1.

H_2 upgrading: As experimentally demonstrated, a C-H-O feedstock will always lead to the formation of reaction byproducts, mostly CO and CO_2. The produced gas will need to be

treated in a post-treatment for the separation and recovery of individual compounds. Figure 13 depicts a separation unit successively removing H_2O vapor, removing CO_2, and carrying out the membrane recovery of H_2. Current membrane modules have a proven H_2 purity and recovery >95%. The detailed design of the upgrading was presented by Deng et al. [44].

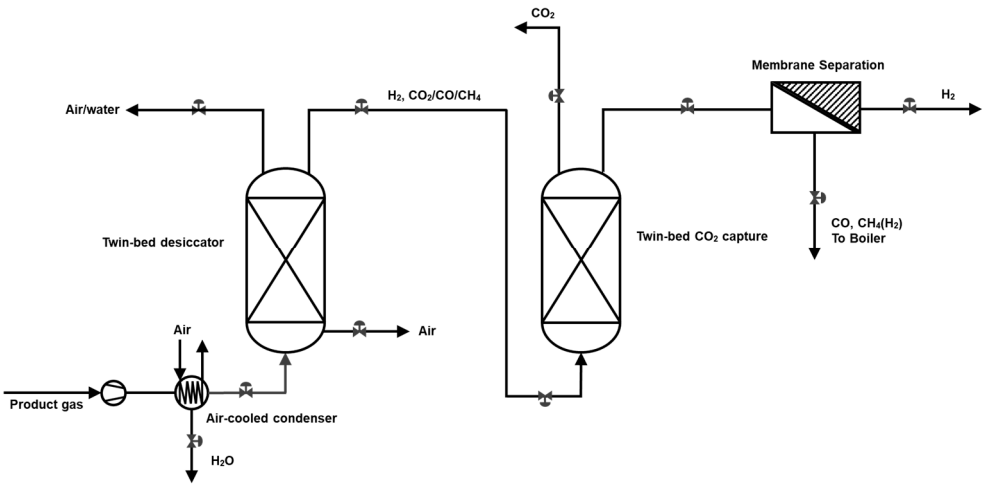

Figure 13. Purification cycles of H_2.

At such high recovery, minor amounts of H_2 will accompany the CO and CH_4 flows, and these flows will be the potential heat source for the feedstock evaporation and preheating.

Safety issues of producing/using H_2: The literature on the safety issues associated with producing and using hydrogen is extensive, and attention is specifically paid to the selection of high-pressure durable materials to counter hydrogen attack, embrittlement, and cracking. The proposed materials differ from high to low pressure storage. While austenitic stainless steel, Al alloys, Cu, and Cu alloys are recommended for their high tensile strength at high pressures, low density, and chemical H_2 inertness, low-pressure vessels can be constructed in AISI 316, 304, 304 L, and 316 L steels. Cu alloys and Al alloys can also withstand H_2 attack.

Redox-driven water splitting results demonstrate that $MnFe_2O_4/Na_2CO_3$ is the ideal redox pair, with a recommended 3 h oxidation cycle (with H_2O) and a 6 h reduction cycle (with collected CO_2). Efficiencies, even after 35 cycles, reach above 90% at 600 °C. Although experiments with $MnFe_2O_4$ were only conducted for long durations at TGA scale, preliminary solar-driven tests were performed during the oxidation cycle. The maximum temperature of the reactor wall in the cavity must be limited to 900 °C (thermo-mechanical strength limits of Incoloy); the bed temperature was kept uniform between 710 and 735 °C by heliostat focusing. The solar H_2 yield at 735 °C was nearly the theoretical H_2 yield of 0.5 mol/mol, as shown in Figure 14. Since the operation requires a twin-reaction mode (oxidation/reduction), both reactors were installed inside the CST cavity. The reactors will be operated in a reversible mode during consecutive cycles (and probably consecutive days). Since the reactor will be of a fixed-bed nature, either a concentrated solar tower or a parabolic dish solar concept can be used.

The Technology Readiness Level (TRL) reflects the development level of a given technology based upon various parameters determined for long-duration applications, such as robustness, reliability, production costs, energy efficiency, and utilization constraints, among others. A hybrid operation mode, with curtailed wind/PV/concentrated solar supplies, seems the obvious solution. Together with heat management within the process, concentrated solar energy from the receiver should be stored and used in periods where cheaper PV electricity is not available (in non-sun periods). Whereas catalytic conversions of appropriate feedstock operate at moderate temperatures, the significantly higher temperatures needed in water splitting are more problematic. At the current stage

of thermo-catalytic or thermo-redox H_2 production, it must be admitted that they only achieve a TRL between 1 and 3.

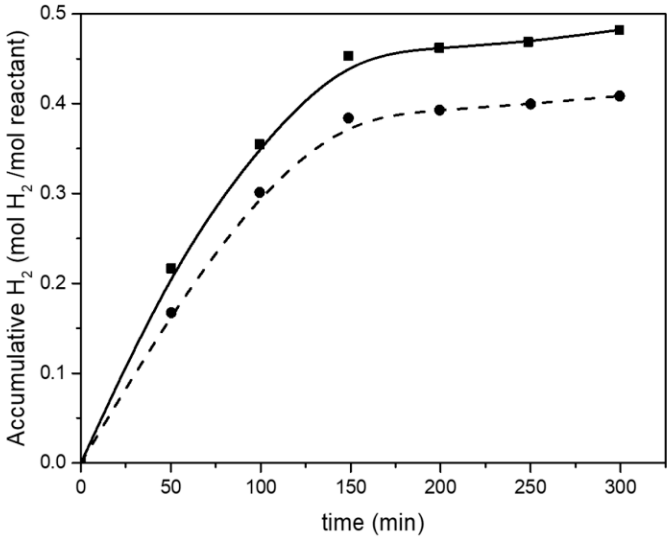

Figure 14. Solar H_2 production using the $MnFe_2O_4/Na_2CO_3$ water splitting cycle at 735 °C (■) and 710 °C (●).

Future cost estimations are extremely challenging, subjective, and inaccurate, mostly because of the low TRLs of the processes. Cost estimations are hence premature. While no solar H_2 production method has achieved a fair TRL so far, further research, preferably pilot- or large-scale research, is urgently needed to help establish the ongoing hydrogen revolution. At present, the state-of-the-art systems only achieve a TRL between 1 and 3.

Techno-economic assessment: Table 1 already included a cost comparison of the different H_2 production methods. A further comparison was made on the basis of the levelized cost of hydrogen (LCOH) and the calculated GHG emissions. Table 7 illustrates this comparison. Developed catalytic feedstock decomposition and redox water splitting offer major advantages.

Table 7. Comparing H_2 production methods (from 2017 to 2023).

	LCOH (USD/kg H_2)	**GHG Emission (kg CO_2-eq/kg H_2)**
Methane steam reforming	1.25	8.5–11
Coal gasification	1.5	12.7–16.8
PEM electrolysis (renewable energy)	7.7	0
Biomass gasification	3 (for large scale) >5 (otherwise)	0 (if biomass is carbon neutral)
Pyrolysis	1.8–2.1	-
Methanol steam reforming	2.2	>3
Ethanol steam reforming	1–2.5	>3
Methane decomposition	0.4–1.5 *	0.85–1.05
Ammonia decomposition	1.5–2.5	0
Redox water splitting	~1.0	0

* Carbon black is sold at EUR 470 and EUR 1870 per ton.

Redox water splitting using the $MnFe_2O_4/Na_2CO_3$ system could achieve a low LCOH (<1 USD/kg H_2) for recyclability for over 120 cycles.

Solar energy as a heat source in particle-driven systems: The Next-CSP receiver is of specific interest in the concentrated solar power technology. Its potential capacity up to 50 MW_{th}, however, exceeds the needs of H_2 production concepts where 100 kW_{th} to 1 MW_{th} would meet the required needs. It is hence important to stress the applicability

of two cheaper concentration technologies: a crossflow fluidized bed receiver, which is installed in the focusing cavity, and the improved solar dish technology, developed by the Chinese Academy of Sciences. Both are currently being tested for water splitting and catalytic ethanol conversions. The small-footprint solar dish system can reach very high temperatures (dictated by the construction materials) and operates at a solar concentration ratio of around 2000.

A 64 m^2 solar dish is depicted in Figure 15. Ongoing developments will help reach 500 m^2, thus allowing for the capturing of 500 kW_{th} at a DNI of 1 kW/m^2. With a 790% dish-to-cavity efficiency and a 75% receiver efficiency, up to ~260 kW_{th} can be used in the ethanol or water splitting reactions.

Figure 15. Novel concentrated solar dish technology developed by the Chinese Academy of Sciences.

The 2025 UN sustainable development goals (SDGs) comprise 17 objectives to be achieved by 2030. The above assessment of the "green" H_2 production methods demonstrates that solar or curtailed renewable energy processes will significantly contribute to meeting these goals [44].

7. Conclusions and Recommendations

The general conclusions of this research review are summarized below:

(i) Renewable energy-based H_2 production from "green" and "gray" feedstock in the presence of steam: the reaction is fast; first-order kinetics and operation at T << 600 °C; near-stoichiometric H_2 yields are achieved; CO, CO_2, and CH_4 are closing the C balance.

(ii) Two priority water splitting redox reactions are favored: $MnOx/Na_2CO_3$ is possible at high T, but recyclability is incomplete. $MnFe_2O_4/Na_2CO_3$ has a high potential. Recyclability for >35 cycles was proven. If >120 cycles can be achieved, the H_2 cost will be <1 USD/kg H_2.

(iii) Thermo-catalytic and thermo-chemical processes can work with heating by excess wind/PV power, preferably with CST for continuous operation.

(iv) Bio-ethanol is attractive since we can accept crude bio-ethanol (after filtration), thus avoiding two distillation steps and the final molecular sieve dewatering, so the price reduction is about 30%.

(v) Ammonia must be further developed since it may be a solution for on-car H_2 generation (ammonia is easy to store). This could also offer possibilities for methanol.

(vi) The design recommendations and tentative economic balances should be proven at pilot scale. This experimental research study provides conclusions that are positive enough to inspire other researchers and even R&D centers to continue this research.

Author Contributions: Methodology, Y.D.; validation, S.L. and H.Z.; data curation, Y.D. and S.L.; writing—original draft preparation, Y.D., J.B. and H.Z.; writing—review and editing, Y.D., J.B., H.L.

and H.Z.; supervision, J.B.; project administration, H.L.; funding acquisition, H.L. All authors have read and agreed to the published version of the manuscript.

Funding: The authors gratefully acknowledge the support of the National Natural Science Foundation of China (NSFC-No. 22208017).

Institutional Review Board Statement: Not applicable.

Informed Consent Statement: Not applicable.

Data Availability Statement: The raw data supporting the conclusions of this article will be made available by the authors on request.

Conflicts of Interest: The authors declare no conflict of interest.

References

1. Pekic, S. *Facts and Factors: Green Hydrogen Market to Grow to $1.423m by 2026*; Offshore Energy: Schiedam, The Netherlands, 2021.
2. Deng, Y.; Dewil, R.; Appels, L.; Van Tulden, F.; Li, S.; Yang, M.; Baeyens, J. Hydrogen-Enriched Natural Gas in a Decarbonization Perspective. *Fuel* **2022**, *318*, 123680. [CrossRef]
3. Li, S.; Zhang, H.; Nie, J.; Dewil, R.; Baeyens, J.; Deng, Y. The Direct Reduction of Iron Ore with Hydrogen. *Sustainability* **2021**, *13*, 8866. [CrossRef]
4. CN CemNet. Buxton Plant Manufactures Industrial Lime with Hydrogen Technology. Available online: https://www.cemnet.com/News/story/173001/buxton-plant-manufactures-industrial-lime-with-hydrogen-technology.html (accessed on 22 July 2022).
5. Lansdorf, T. Hydrogen—A Game Changer for the Ceramic Industry. *Interceram-Int. Ceram. Rev.* **2022**, *71*, 48–54. [CrossRef]
6. Chelvam, K.; Hanafiah, M.M.; Woon, K.S.; Ali, K. Al A Review on the Environmental Performance of Various Hydrogen Production Technologies: An Approach towards Hydrogen Economy. *Energy Rep.* **2024**, *11*, 369–383. [CrossRef]
7. Antweiler, W. What Role Does Hydrogen Have in the Future of Electric Mobility? Available online: https://wernerantweiler.ca/blog.php?item=2020-09-28 (accessed on 4 January 2024).
8. Abdin, Z.; Zafaranloo, A.; Rafiee, A.; Mérida, W.; Lipiński, W.; Khalilpour, K.R. Hydrogen as an Energy Vector. *Renew. Sustain. Energy Rev.* **2020**, *120*, 109620. [CrossRef]
9. BP p.l.c. Hydroelectricity. Available online: https://www.bp.com/en/global/corporate/energy-economics/statistical-review-of-world-energy/hydroelectricity.html (accessed on 4 January 2024).
10. Minutillo, M.; Perna, A.; Sorce, A. Combined Hydrogen, Heat and Electricity Generation via Biogas Reforming: Energy and Economic Assessments. *Int. J. Hydrogen Energy* **2019**, *44*, 23880–23898. [CrossRef]
11. Kazi, M.-K.; Eljack, F.; El-Halwagi, M.M.; Haouari, M. Green Hydrogen for Industrial Sector Decarbonization: Costs and Impacts on Hydrogen Economy in Qatar. *Comput. Chem. Eng.* **2021**, *145*, 107144. [CrossRef]
12. Chi, J.; Yu, H. Water Electrolysis Based on Renewable Energy for Hydrogen Production. *Chin. J. Catal.* **2018**, *39*, 390–394. [CrossRef]
13. Shiva Kumar, S.; Himabindu, V. Hydrogen Production by PEM Water Electrolysis—A Review. *Mater. Sci. Energy Technol.* **2019**, *2*, 442–454. [CrossRef]
14. Idriss, H. Hydrogen Production from Water: Past and Present. *Curr. Opin. Chem. Eng.* **2020**, *29*, 74–82. [CrossRef]
15. Bhandari, R.; Trudewind, C.A.; Zapp, P. Life Cycle Assessment of Hydrogen Production via Electrolysis—A Review. *J. Clean. Prod.* **2014**, *85*, 151–163. [CrossRef]
16. Ursua, A.; Gandia, L.M.; Sanchis, P. Hydrogen Production from Water Electrolysis: Current Status and Future Trends. *Proc. IEEE* **2012**, *100*, 410–426. [CrossRef]
17. Hino, R.; Haga, K.; Aita, H.; Sekita, K. R&D on Hydrogen Production by High-Temperature Electrolysis of Steam. *Nucl. Eng. Des.* **2004**, *233*, 363–375. [CrossRef]
18. Deng, Y.; Dewil, R.; Appels, L.; Li, S.; Baeyens, J.; Degrève, J.; Wang, G. Thermo-Chemical Water Splitting: Selection of Priority Reversible Redox Reactions by Multi-Attribute Decision Making. *Renew. Energy* **2021**, *170*, 800–810. [CrossRef]
19. Nemitallah, M.A.; Alnazha, A.A.; Ahmed, U.; El-Adawy, M.; Habib, M.A. Review on Techno-Economics of Hydrogen Production Using Current and Emerging Processes: Status and Perspectives. *Results Eng.* **2024**, *21*, 101890. [CrossRef]
20. Chao, C.; Deng, Y.; Dewil, R.; Baeyens, J.; Fan, X. Post-Combustion Carbon Capture. *Renew. Sustain. Energy Rev.* **2021**, *138*, 110490. [CrossRef]
21. Licht, S. Over 18% Solar Energy Conversion to Generation of Hydrogen Fuel; Theory and Experiment for Efficient Solar Water Splitting. *Int. J. Hydrogen Energy* **2001**, *26*, 653–659. [CrossRef]
22. Hara, D. Toward a Hydrogen Society—Introduction of Representative Projects in Japan. *ECS Trans.* **2019**, *91*, 3–7. [CrossRef]
23. Arribas, L.; González-Aguilar, J.; Romero, M. Solar-Driven Thermochemical Water-Splitting by Cerium Oxide: Determination of Operational Conditions in a Directly Irradiated Fixed Bed Reactor. *Energies* **2018**, *11*, 2451. [CrossRef]
24. Klahr, B.M.; Peterson, D.; Randolph, K.; Miller, E.L. Innovative Approaches to Addressing the Fundamental Materials Challenges in Advanced Water Splitting Technologies for Renewable Hydrogen Production. *ECS Trans.* **2017**, *75*, 3–11. [CrossRef]

25. Herdem, M.S.; Sinaki, M.Y.; Farhad, S.; Hamdullahpur, F. An Overview of the Methanol Reforming Process: Comparison of Fuels, Catalysts, Reformers, and Systems. *Int. J. Energy Res.* **2019**, *43*, 5076–5105. [CrossRef]
26. Moraes, T.S.; Cozendey da Silva, H.N.; Zotes, L.P.; Mattos, L.V.; Pizarro Borges, L.E.; Farrauto, R.; Noronha, F.B. A Techno-Economic Evaluation of the Hydrogen Production for Energy Generation Using an Ethanol Fuel Processor. *Int. J. Hydrogen Energy* **2019**, *44*, 21205–21219. [CrossRef]
27. Liu, J.; Li, S.; Dewil, R.; Vanierschot, M.; Baeyens, J.; Deng, Y. Water Splitting by $MnOx/Na_2CO_3$ Reversible Redox Reactions. *Sustainability* **2022**, *14*, 7597. [CrossRef]
28. Shaner, M.R.; Atwater, H.A.; Lewis, N.S.; McFarland, E.W. A Comparative Technoeconomic Analysis of Renewable Hydrogen Production Using Solar Energy. *Energy Environ. Sci.* **2016**, *9*, 2354–2371. [CrossRef]
29. Kolb, G.J.; Diver, R.B.; Siegel, N. Central-Station Solar Hydrogen Power Plant. *J. Sol. Energy Eng.* **2007**, *129*, 179–183. [CrossRef]
30. Zhang, Y.; Wang, Z.; Du, Z.; Li, Y.; Qian, M.; Van Herle, J.; Wang, L. Techno-Economic Analysis of Solar Hydrogen Production via PV Power/Concentrated Solar Heat Driven Solid Oxide Electrolysis with Electrical/Thermal Energy Storage. *J. Energy Storage* **2023**, *72*, 107986. [CrossRef]
31. Xue, X.; Han, W.; Xin, Y.; Liu, C.; Jin, H.; Wang, X. Proposal and Energetic and Exergetic Evaluation of a Hydrogen Production System with Synergistic Conversion of Coal and Solar Energy. *Energy* **2023**, *283*, 128489. [CrossRef]
32. Hosseini, S.E.; Wahid, M.A. Hydrogen from Solar Energy, a Clean Energy Carrier from a Sustainable Source of Energy. *Int. J. Energy Res.* **2020**, *44*, 4110–4131. [CrossRef]
33. Charvin, P.; Stéphane, A.; Florent, L.; Gilles, F. Analysis of Solar Chemical Processes for Hydrogen Production from Water Splitting Thermochemical Cycles. *Energy Convers. Manag.* **2008**, *49*, 1547–1556. [CrossRef]
34. Zoller, S.; Koepf, E.; Nizamian, D.; Stephan, M.; Patané, A.; Haueter, P.; Romero, M.; González-Aguilar, J.; Lieftink, D.; de Wit, E.; et al. A Solar Tower Fuel Plant for the Thermochemical Production of Kerosene from H_2O and CO_2. *Joule* **2022**, *6*, 1606–1616. [CrossRef]
35. Khormi, N.A.; Fronk, B.M. Feasibility of High Temperature Concentrated Solar Power for Cogeneration of Electricity and Hydrogen Using Supercritical Carbon Dioxide Receiver Technology. In Proceedings of the ASME 2023 17th International Conference on Energy Sustainability, American Society of Mechanical Engineers, Washington, DC, USA, 10–12 July 2023.
36. Lampe, J.; Menz, S. Optimized Operational Strategy of a Solar Reactor for Thermochemical Hydrogen Generation. *Optim. Eng.* **2024**, *25*, 29–61. [CrossRef]
37. Dong, W.J.; Ye, Z.; Tang, S.; Navid, I.A.; Xiao, Y.; Zhang, B.; Pan, Y.; Mi, Z. Concentrated Solar Light Photoelectrochemical Water Splitting for Stable and High-Yield Hydrogen Production. *Adv. Sci.* **2024**. *early view*. [CrossRef] [PubMed]
38. Bentoumi, L.; Miles, A.; Korei, Z. Green Hydrogen Production by Integrating a Solar Power Plant with a Combined Cycle in the Desert Climate of Algeria. *Sol. Energy* **2024**, *268*, 112311. [CrossRef]
39. Herrando, M.; Wang, K.; Huang, G.; Otanicar, T.; Mousa, O.B.; Agathokleous, R.A.; Ding, Y.; Kalogirou, S.; Ekins-Daukes, N.; Taylor, R.A.; et al. A Review of Solar Hybrid Photovoltaic-Thermal (PV-T) Collectors and Systems. *Prog. Energy Combust. Sci.* **2023**, *97*, 101072. [CrossRef]
40. Benghanem, M.; Mellit, A.; Almohamadi, H.; Haddad, S.; Chettibi, N.; Alanazi, A.M.; Dasalla, D.; Alzahrani, A. Hydrogen Production Methods Based on Solar and Wind Energy: A Review. *Energies* **2023**, *16*, 757. [CrossRef]
41. Liu, J.; Wang, J.; Tang, Y.; Jin, J.; Li, W. Solar Photovoltaic–Thermal Hydrogen Production System Based on Full-Spectrum Utilization. *J. Clean. Prod.* **2023**, *430*, 139340. [CrossRef]
42. Boudries, R. Techno-Economic Study of Hydrogen Production Using CSP Technology. *Int. J. Hydrogen Energy* **2018**, *43*, 3406–3417. [CrossRef]
43. IEA. The Future of Hydrogen. 2019. Available online: https://www.iea.org/reports/the-future-of-hydrogen (accessed on 1 February 2024).
44. Deng, Y.; Li, S.; Appels, L.; Zhang, H.; Sweygers, N.; Baeyens, J.; Dewil, R. Steam Reforming of Ethanol by Non-Noble Metal Catalysts. *Renew. Sustain. Energy Rev.* **2023**, *175*, 113184. [CrossRef]
45. Deng, Y.; Li, S.; Dewil, R.; Appels, L.; Yang, M.; Zhang, H.; Baeyens, J. Water Splitting by $MnFe_2O_4/Na_2CO_3$ Reversible Redox Reactions. *RSC Adv.* **2022**, *12*, 31392–31401. [CrossRef]